Characterization of Rhodamine 6G Aggregates Intercalated in Solid Thin Films of Laponite Clay. 2 Fluorescence Spectroscopy

V. Martínez Martínez, F. López Arbeloa,* J. Bañuelos Prieto, and I. López Arbeloa

Departamento de Química Física, Universidad del País Vasco-EHU, Apartado 644, 48080-Bilbao, Spain

Received: January 25, 2005; In Final Form: February 4, 2005

The photoluminescence response of Rhodamine 6G (R6G) laser dye intercalated into solid thin films of Laponite (Lap) clay is studied as a function of dye loading. Fluorescence spectroscopy (steady-state and time-resolved techniques) was used to characterize the R6G species adsorbed into the solid films. For very diluted R6G loadings (≤0.1% CEC, i.e., the percentage of the total cation exchange capacity of Lap) the fluorescence properties of R6G monomer were characterized, which presents an emission band centered at 548 nm, an average lifetime of 4.2 ns, and a fluorescence efficiency higher than that of the R6G monomer in liquid solution. By increasing the loading, dye molecules tend to self-aggregate, and different dimers are formed in moderate dye concentrations (in the 1−25% CEC range): oblique head-to tail J-type dimers, with weak emission bands at around 575 nm; and sandwich H-type dimers, as efficient quenchers of the fluorescent emission. Higher-order aggregates of R6G in Lap films are formed in high loading samples (>40% CEC), with a reminiscent fluorescence band at around 600 nm.

Introduction

Nowadays, the designing of optical materials is an important research field for the development of functional photonic devices with important technological applications such as solid-state dye lasers, chemical sensors, optical storage devices, antenna systems, solar cells and so on.[1−15] The encapsulation of organic laser dyes in different solid host materials,[1−4,16−19] mainly inorganic matrixes, can provide high-quality photoluminescence materials, not only improving the laser performance (tunability and efficiency) but also increasing the thermal- and photostability of the dyes. Moreover, the adsorption of the photoactive molecules in highly prearranged architectures in the nanometer scales allows the development of the optical nanocomposite materials with a preferential orientation of the guest molecules.[20−31] In this sense, layered clay minerals are interesting hosts for the incorporation of dye molecules due to their great adsorption capacities (both high cation exchange capacity and high area/volume ratio) and the ability to build up 2D-organized structures (stacking of the layers giving rise to an accessible interlayer space in the nanometer scale).[32,33] The adsorption of dye molecules in parallel bidimensional arrangements of the clay particles (for instance, in supported thin films) gives rise to a macroscopic distribution of the dye molecules with a preferential orientation into the interlayer space of the host material.[6,19,21,34−38]

For customizing optical materials with a required aim, the photophysics of the adsorbed dye molecules in the host matrix should be characterized. The photophysical properties of the dye molecules adsorbed in solid surfaces would depend not only on the physicochemical properties of the matrix (i.e., polarity, refractive index, acidity, etc.), but also on the host−guest interactions, affecting the distribution and orientation of the dye molecules on the host material, as well as on the dye-dye interactions, responsible for the dye aggregation.[1,22,35]

SCHEME 1: Exciton Splitting of the Electronic Excited States for Different Geometric Dispositions of the Monomer Units in the Dimer[a]

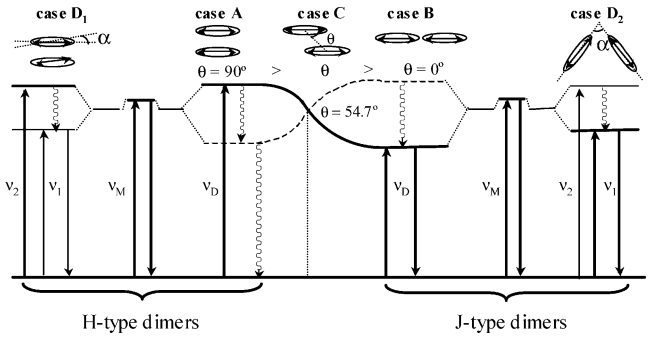

[a] Linear arrows, radiative transitions; waved arrows, nonradiative transitions.

Indeed, high optical density samples of dye are required to record the laser signal. Under these conditions, dye molecules have a high tendency to self-associate, drastically decreasing the fluorescent emission of the samples, since the dye-aggregates have non- or poor emission capacity and they are efficient quenchers of the fluorescent emission from the monomers. For this reason, the reduction in the dye aggregation by the encapsulation of the dye molecules into host material should be of interest to develop tunable dye lasers in the solid state.[1−3,11,39]

The exciton theory,[41,42] a molecular quantum mechanical theory based on monomer dipole−dipole interaction in the aggregates predicts a splitting of the excited state, changing the spectroscopic characteristics of the dimers. Thus, the absorption and fluorescence properties of the dimers depend on the geometrical distribution of the monomer units in the aggregate (see Scheme 1). In the perfect so-called H-dimer, in which the monomer units are disposed in parallel planes as a sandwich-

* Corresponding author. Address: Departamento de Química Física, Universidad del País Vasco, EHU, Apartado 644, 48080-Bilbao, Spain. Phone: +34 94 601 59 71. Fax: +34 94 464 85 00. E-mail: qfploarf@lg.ehu.es.

10.1021/jp050440i CCC: $30.25
Published on Web 03/16/2005

like structure (case A), only the transition to the highest excited state is allowed in absorption and the deactivation to the ground state via the lowest excited state should be not fluorescent. However, a disruption of this structure with a twisted angle α between the monomers (the so-called twisted sandwich H-type dimer, case D_1 in Scheme) would involve a dimer with an emission band placed at lower energies than the monomer fluorescence band, although its transition moment would depend on the distortion α angle. Indeed, the fluorescence intensity should be negligible when the α angle tends to 0. Consequently and depending on the α value, these dimers can act as efficient quenchers for the monomer emission. On the other hand, linear head-to-tail dimers (Case B), coplanar-displacement dimers (case C) with an angle $\theta < 54.7°$, or oblique head-to-tail dimers (case D_2), all of them called J-type dimers, are characterized by emission bands placed at lower energy than the monomeric fluorescent band, and an emission capacity which will depend on the final geometrical disposition of the monomer units in the aggregate (θ and α angles).

In the present paper, the photoluminescence properties of Rhodamine 6G, probably the most-used laser dye, in solid thin films of Laponite clay (Lap), a smectite-type clay with a high affinity to adsorb organic dyes,[43] are described. Previously, the morphology and the distribution of Lap films supported on glass were checked by atomic force and scanning electron microscopies.[44] The incorporation of R6G molecules in the interlayer space of Lap films was confirmed by the X-ray diffraction technique, elemental CHN analysis and electronic spectroscopies.[44]

The R6G aggregation in Lap films was also studied by electronic absorption spectroscopy.[45] The evolution of the absorption spectra of R6G/Lap films with the dye loading revealed an aggregation process of the dye adsorbed on the clay surface. For very diluted dye/clay films, ≤0.1% CEC (defined as the percentage of the total cation exchange capacity of the clay, CEC), the dye was adsorbed as monomeric units, and the dye aggregation is negligible. R6G dimers were observed in moderate dye loading samples (1−25% CEC). Since these aggregates present two absorption bands at both sides of the monomer absorption band, the band placed at longer wavelengths being more intense, an oblique R6G dimer in Lap films was characterized, although the presence of other types of dimers was not excluded. High-order R6G aggregates in Lap films, characterized by an absorption band at shorter wavelengths, were observed for high loading samples (>40% CEC). The coexistence of different kinds of aggregates is a common phenomenon in solid-state samples due to the microheterogeneity in the physicochemical properties of the host, the morphology of the host architecture and the relative distribution and orientation of the guest molecules.[46−55]

The photoluminescence properties of R6G/Lap films are now studied. Both steady state and time-resolved fluorescent techniques are used to obtain a better characterization of the R6G aggregates in Lap films.

Experimental Section

Rhodamine 6G (R6G, Laser Grade) was purchased by Kodak and was used as received. Synthetic Laponite clay (Lap) in its sodium form supplied by Laporte Industries, is characterized by a high purity, very small particle size (∼0.03 μm) and the ability to provide high dispersed aqueous suspensions.[33] The spin coating technique was applied to obtain Lap films supported on glasses by dropping an aqueous Lap suspension (2% in weight) on the substrate. The thickness (around 250 nm) was controlled by the spinning conditions (2500 rpm, 60 s), and the morphology and the orientation of the clay particles in the films were analyzed by atomic force microscopy, as described previously.[44] The intercalation of the dye was conducted by immersing the Lap films in a water/ethanol solution of R6G with a water molar fraction, x_w, of 0.8. The loading of the dye on the film was adjusted by the dye concentration (10^{-5} or 10^{-3} M) and the immersion time (from 5 min to 2 days). After intercalation, the samples were rinsed with ethanol and water, and they were dried overnight in an airflow oven at 35 °C. Finally, and in order to get an adequate redistribution of the adsorbed R6G molecules in the Lap films, the samples were kept in darkness for 2 days. Further details for the optimal preparation of R6G/Lap films are discussed elsewhere.[44]

Excitation and emission spectra were recorded on a Shimadzu RF-5000 spectrofluorimeter in a front-face configuration by a solid sample holder. To reduce the detection of the excitation light scattering by the samples, the films were oriented with the normal to the substrate at 40° and 50° with respect to the excitation beam and the detection channel, respectively. Excitation spectra were recorded at an emission wavelength of 600 nm with excitation and emission slits of 3 and 5 nm, respectively, and were corrected for the excitation intensity at any wavelength. Emission spectra were registered, after excitation at 495 nm, with excitation and emission slits of 5 and 3 nm, respectively, and were corrected for the monochromator and photomultiplier response functions. Both excitation and emission spectra were corrected from the scattering of the excitation radiation by subtracting the corresponding signal obtained for a Lap film without dye.

Radiative deactivation curves were recorded by means of the time-correlated single-photon counting technique (Edinburgh Instruments, model FL 920). This instrument is equipped with an emission double monochromator and has a time resolution of 30 ps after deconvolution of the excitation pulse. The excitation was performed by diode laser (PicoQuant, model LDH 410) at 410 nm with pulses of 150 ps FWMH, a repetition rate of 40 MHz and an excitation power of 0.65 mW. The emission signal was detected in a similar front-face configuration to that described in the fluorimeter (40° and 50° with respect to the excitation and emission arms), but the substrates were leaned back 30° with respect to the plane formed by the excitation and emission beams. The erratic scattering signal of the laser was avoided in the detection channel by filtering the excitation light with a 450 nm cutoff filter. From the recorded fluorescent decay curves, two different analysis can be performed of the recorded data considering two experimental setups:

(i) Lifetime analysis. For a fixed emission wavelength, the fluorescence decay curve was collected up to10000 counts at the channel with the maximum emission. The lifetime of the samples was obtained from the recorded decay curves after deconvolution of the instrument response function (IRF) carried out by an iterative method of nonlinear least-squares based on the Marquardt algorithm. The IRF signal was collected with a Lap film without dye at 410 nm. The decay curves were adjusted to a sum of exponential decays (i.e., as multiexponentials) by means of:

$$I_{flu}(t) = A_1 \exp(-t/\tau_1) + A_2 \exp(-t/\tau_2) + ... \qquad (1)$$

where A_i are the preexponential factors related with the statistical weights of each exponential and τ_i are the lifetimes of each exponential decay. The goodness of the deconvolution process was controlled by the chi-squared (χ^2) and Durbin-Watson (D.W.) statistical parameters and the residual analysis. The

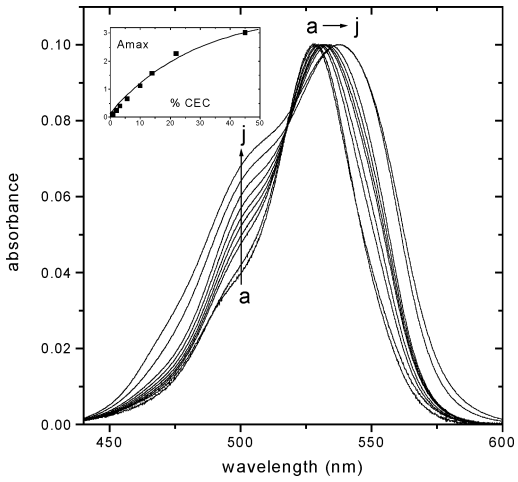

Figure 1. Height-normalized absorption spectra of R6G adsorbed in Lap films for different relative dye/clay concentrations (in % CEC): 0.1 (a), 1.0 (b), 2.0 (c), 3.2 (d), 5.7 (e), 10 (f), 14 (g), 22 (h), 45 (i), and 60 (j).

fluorescence decay curves were analyzed at at least two emission wavelength: 550 and 580 nm.

(ii) Time-resolved emission spectra (TRES). Fluorescence decay curves were recorded as a function of the emission wavelength in the 520−650 nm range (wavelength increment of 2 nm) for a fixed recording time (200 s per wavelength). The emission spectra at different times after excitation were obtained by averaging the integrated fluorescence intensity for fixed time-windows of 0.125 ns at every wavelength in the 0−2.5 ns time interval (20 time-window spectra) after the excitation pulse.

Results and Discussion

In a previous paper,[45] the metachromasy effect observed in the absorption spectra of R6G/Lap film by changing the dye loading (Figure 1) was ascribed to the dye aggregation. For very low loading samples (≤0.1% CEC), R6G molecules are adsorbed as monomer units with an absorption spectrum (curve a in Figure 1) similar to that observed in a diluted ($\sim 2 \times 10^{-6}$ M) solution of R6G in ethanol.[56] For moderated R6G/Lap loadings, i.e., in the 1−25% CEC range, the main absorption band, centered at 528 nm, progressively shifts to higher wavelengths and the relative intensity at the vibronic shoulder, around 500 nm, increases (Figure 1). These results are consistent with the formation of an oblique head-to-tail dimer, although the presence of other type of dimers cannot be excluded. Indeed, the shape of the calculated adsorption spectrum for the aggregate evolutes with the dye concentration in this loading range;[45] for instance, the relative intensity of the absorption band of the dimer at higher wavelengths (∼545 nm) over that at lower wavelengths (∼504 nm) decreases as the amount of R6G on Lap increases. For higher-loading R6G/Lap samples (>40% CEC), a progressive increase in the absorbance at around 475 nm was ascribed to the formation of a high-order aggregate (Figure 1, curves i−j), although it was not spectroscopically characterized because of the presence of several aggregates (dimers, trimers, ...). In the present paper, fluorescence techniques are applied to obtain extra information on the aggregation of R6G in Lap films and to characterize the photophysical properties of R6G dye adsorbed in solid Lap films.

Figure 2A shows the height-normalized fluorescence spectra of R6G in Lap films for different loadings (0.1−40% CEC). By increasing the dye concentration, a gradual shift from 548 to 586 nm is observed in the emission band, together with a drastic loss in the fluorescence capacity (inset in Figure 2A). Several authors have assigned the observed red shift in the fluorescence band of rhodamine dyes in different Langmuir Blodgget (LB) films to a distribution of the angle between the phenyl ring and the xanthene plane of rhodamine as a consequence of the restricted space of LB films.[53−55,57,58] However, this is not the present case, since similar bathochromic shifts should be observed in both the absorption and the emission bands and the effect should be independent of the dye concentration. Therefore, the spectral shift observed in Figure 2A should be attributed to other factors: the inner filter effects (i.e., high absorption of the excitation light and the reabsorption phenomenon) in high dye concentration samples;[59,60] changes in the environment polarity by the presence of organic dye molecules in the interlayer space of Lap films[61,62] and the fluorescent emission from the R6G aggregates.[41,42] Although the two former factors cannot be excluded, their contribution probably cannot explain such a drastic shift in the fluorescence band. Indeed, the inner filter effects should be negligible for the dye concentration and the front-face configuration used in the present work. The thickness of the films was also adjusted in order to obtain samples with absorbance at the excitation wavelength no higher than 1. On the other hand, the changes in the environment polarity would not explain the drastic loss observed in the fluorescence intensity (inset in Figure 2A). Moreover, the observed fluorescence spectral shift of the 1% CEC sample could not be assigned to changes in the environment polarity since the high dispersion of the adsorbed dye molecules in these diluted R6G films would not affect the photophysical properties of individual R6G molecules. Hence, the spectral shift in the fluorescence band should be ascribed to the emission from R6G aggregates in the interlayer space of Lap films.

This conclusion is confirmed by excitation spectra (Figure 2B), recorded at the lower-energy part ($\lambda_{flu} \approx 600$ nm) of the fluorescence band. For the highest diluted R6G/Lap films (0.1% CEC), the narrow excitation band (curve a in Figure 2B) is similar to the absorption spectrum of the R6G monomer (curve a in Figure 1). However, by increasing the R6G concentration, the excitation spectra progressively shift to lower energies, confirming the fluorescent emission of R6G aggregates on Lap films at lower energies than de monomer emission. Moreover, the shape of these excitation spectra, with a main absorption band at higher wavelengths and a shoulder at lower wavelengths, suggests the formation of oblique head-to-tail type aggregates, as was previous concluded by absorption spectroscopy.[45]

The fluorescent emission of R6G aggregates should be very low, because of the severe loss in the fluorescent intensity of the R6G/Lap films with the dye loading (inset Figure 2A). Moreover, R6G aggregates should be very efficient quenchers for the monomeric emission, since, for instance, the monomeric band in the excitation spectra for the 1% CEC sample practically disappears (curve b in Figure 2B), whereas it is the predominant band in the absorption spectrum (curve b in Figure 1). To characterize the photophysical properties of several R6G species in Lap films, the fluorescence characteristics at different CEC loadings are now analyzed. The fluorescent properties of representative R6G/Lap films are summarized in Table 1.

Considering previous conclusions from the absorption spectra,[45] the monomer of R6G in Lap films can be identified in the most diluted sample (0.1% CEC). The fluorescence band of this sample (curve a in Figure 2A) is similar to that of diluted solutions of R6G in ethanol, but shifted around 4 nm (Table 1) to higher energies. Bathochromic spectral shifts are observed

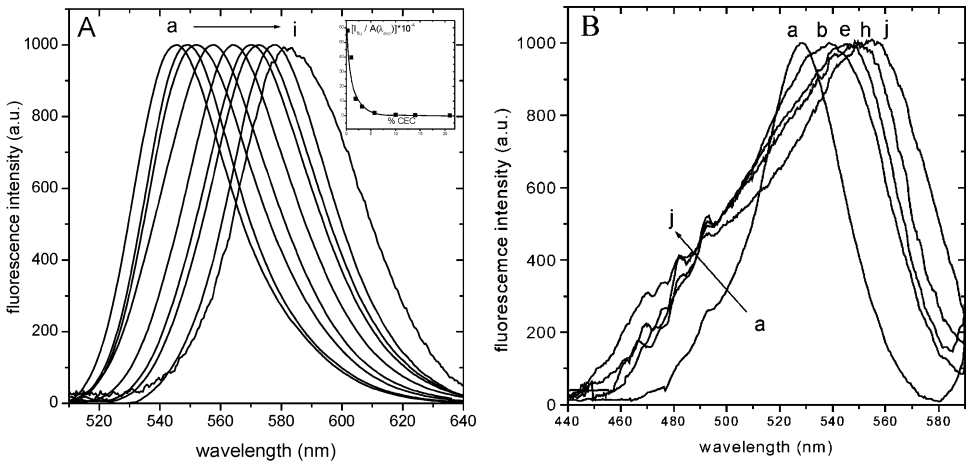

Figure 2. Height-normalized emission (A) and excitation (B) spectra of R6G/Lap films for different relative loadings (see legend in Figure 1). The evolution of the fluorescence intensity over the absorbance at the excitation wavelength with the dye loading I_{flu}/A_{exc}, is shown in the inset.

TABLE 1: Absorption and Fluorescence Parameters of R6G Dye in Lap Films as Function of the Dye Loading (% CEC). The Spectroscopic Characteristics of R6G in Diluted Solutions Are Also Included for Comparison

	λ_{abs} (±0.2 nm)	$\Delta\upsilon_{abs}{}^{a}$ (cm^{-1})	λ_{flu} (±0.5 nm)	$\Delta\upsilon_{flu}{}^{a}$ (cm^{-1})	I_{flu}/A_{exc} (a.u)	$\Delta\nu_{st}$ (cm^{-1})	λ_{exc} (±1 nm)	$\langle\tau_{flu}\rangle_1{}^{b}$ (ns)	$\langle\tau_{flu}\rangle_2{}^{b}$ (ns)
R6G/ethanol[c]	530	1100	552	930	6.5×10^8	750	531	3.85	3.85
R6G/water[c]	527	1270	551	970	4.9×10^8	840	527	3.95	3.95
% CEC					R6G/Lap films				
0.1[c]	528.5	1445	548	1150	9.0×10^8	675	528	4.2	4.5
1[c,d]	529.0	1440	553	1270	5.0×10^8	820	538	3.7	4.4
2[d]	529.7	1754	557	1350	1.2×10^8	925	–	–	–
3.2[d]	530.5	1890	562	1400	7.8×10^7	1050	–	–	–
5.7[d]	531.5	2028	568	1320	2.6×10^7	1320	545	1.6	2.5
10[d]	532.7	2100	573	1315	8.0×10^6	1320	–	–	–
22[d,e]	533.5	2291	580	1210	1.6×10^6	1500	549	0.45	0.65
45[e]	537.0	2558	586	1330	4.4×10^5	1440	–	0.85	0.95
60[e]	538.0	2718	596	1600	2.1×10^5	1495	554	0.98	0.97

[c−e] Major R6G species: [c]monomer, [d]dimers, [e]higher-aggregates. [a] FWMH: full width at the medium height. [b] Mean lifetime obtained from the "intensity average lifetime" (eq 2) and "amplitude average lifetime" (eq 3): $^1\lambda_{em} < 580$ nm; $^2\lambda_{em} > 580$ nm.

in the corresponding absorption and excitation spectra and they can be attributed to the changes in the physicochemical properties of the Lap surfaces with respect to the ethanol surroundings. On the other hand, the adsorption of R6G monomer on Lap films would lead to an increase in the fluorescence quantum yield, since the fluorescence efficiency, analyzed as the ratio between the observed fluorescence intensity and the absorbance at the excitation wavelength (I_{flu}/A_{exc}), is higher for the 0.1% CEC sample than in diluted solutions of R6G in water and ethanol (Table 1). This result is consistent with a reduction of the nonradiative deactivation process from the fluorescent excited state of R6G in rigid media, and is one of the factors to be considered in the development of new tunable dye lasers in the solid state.[4−6] A more rigid and constrained environment reduces the internal mobility and the flexibility of aromatic systems, decreasing the internal conversion processes and improving their fluorescence quantum yield, and consequently their laser efficiency.

However, the fluorescence band of R6G monomer adsorbed in Lap film is wider than that in liquid solutions ($\Delta\nu_{flu}$ in Table 1). This is a general observation of dyes in solid-state samples and is ascribed to changes in the vibronic structure of the electronic band in rigid media. Moreover, in the case of rhodamine dyes, a distribution of the angle between the phenyl ring with respect the main plane of the molecule, as a consequence of the restricted interlayer space at the Lap clay, could contribute to the widening of the fluorescence band. In this case, a distribution of energies sites for the excited state of the monomer with different energy emissions can exist.[53−55,57,58] This argument is consistent with the fluorescence decay curves, since they cannot be analyzed as monoexponential decay curves for the most diluted 0.1% CEC R6G/Lap film. Indeed, three or four exponentials ($\chi^2 \leq 1.10$) are required to deconvolute the evolution of the fluorescence intensities with the time after excitation. Muliexponential decays of rhodamines have been also reported in Langmuir-Blodget (LB) films.[61,62] This multiexponential behavior cannot be ascribed to a reorientation of the monomer and surrounding molecules during the lifetime after excitation because identical decay curves were recorded by using a magic angle configuration, i.e., using an emission polarizer twisted 54.7° with respect to that of the excitation beam (nonshown data). Moreover, the fluorescence curves recorded with horizontal and vertical polarization (nonshown data) remain identical, suggesting the lack of any reorientation of the adsorbed dye molecules and the absence of any preferential orientation with respect to the polarized excitation light during the excited-state lifetime.

The multiexponential decay curves are usually observed in solid samples and they can be attributed to the highly heterogeneous environments for the dye molecules in the solid surfaces.[23,63] Indeed, R6G molecules can interact with the clay surface by several mechanisms;[64] through exchangeable cations; through the interlayer water (both the solvation-shells of the interlayer cations and outside of the coordination sphere); and through the O atoms of the 001 surface of the clay. Because of the difficulty to give an appropriate interpretation for 3- or

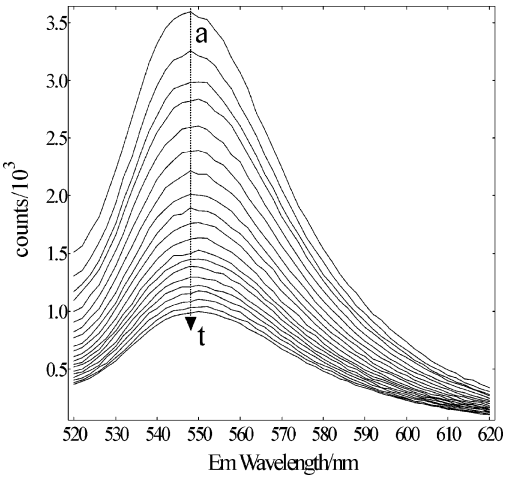

Figure 3. Time-resolved emission spectra for the 0.1% CEC R6G/Lap sample. Spectra were recorded from 0 (curve a) to 2.5 ns (curve t) time after excitation at every 0.125 ns intervals (20 time-window spectra).

4-exponential decay curves, an average lifetime was estimated by means of:[65]

$$\langle\tau\rangle = \frac{\sum A_i \tau_i^2}{\sum A_i \tau_i} \quad (2)$$

where A_i has been defined in eq 1. This "intensity average lifetime" represents the average time in which the molecules are in the excited state.[65,66] However its evaluation overestimated the long lifetime tail component of the obtained fluorescence decay curves, which could be corrected in some extent considering also the "amplitude average lifetime", defined by:

$$\langle\tau\rangle = \sum A_i \tau_i \quad (3)$$

which symbolizes the area under the fluorescence decay curve. The tabulated lifetimes, $\langle\tau_{flu}\rangle$, are the mean values of these two average lifetimes.

The average lifetime of the 0.1% CEC sample at the emission maximum ($\langle\tau_{flu}\rangle_{550} = 4.2$ ns, Table 1) is slightly longer than that of R6G monomers in ethanolic solution ($\tau_{flu} = 3.85$ ns).[67] This result is consistent with the increase in the fluorescence efficiency of R6G monomers in solid samples above-mentioned, confirming the reduction in the nonradiative deactivation of R6G monomer in clay surfaces.

Time-resolved emission spectra of the 0.1% CEC sample (Figure 3) reveal that the fluorescence band does not undergo spectral shifts with the time after excitation. These results rule out the presence of several R6G species with different emission wavelengths and lifetimes. Therefore, the emission characteristics of this diluted 0.1% CEC R6G/Lap film, are assigned to a distribution of the fluorescent excited state of R6G monomers through different parts of the interlayer space of Lap films.

Dimers of R6G on Lap films were characterized by absorption spectroscopy in moderate loadings, in the 1−22% CEC range.[45] The clear isobestic point observed in the absorption spectra in these low-moderate R6G/Lap loadings led us to consider, in a first approximation, the equilibrium of R6G monomer units with a R6G dimer in the 1−22% CEC loading range. However, the absence of a second isobestic point and the slight evolution in the shape of the calculated absorption spectra of the dimer with the R6G loading led us to consider also the presence of other types of R6G dimers in Lap films in this loading range. For a better characterization of these species, their fluorescence properties are now analyzed.

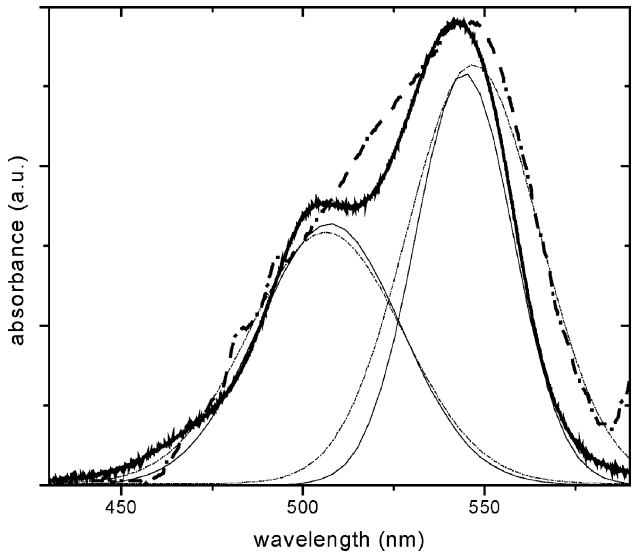

Figure 4. Calculated absorption spectrum of R6G dimer in Lap films in moderated (1−25% CEC) loadings[45] (solid curve) and excitation spectrum of R6G in Lap for the 5.7% CEC (dashed curve). Both spectra are deconvoluted in two Gaussian bands (narrow lines).

The fluorescent band of R6G in Lap films shift to longer wavelengths with the dye loading (Figure 2A), suggesting that the fluorescent state of the dimers is placed at lower energies than the monomer excited state. Similar arguments have been claimed for LB films.[61,62] This conclusion is consistent with the formation of an oblique head-to-tail (D_2) or a coplanar displaced (C) J-type dimers and/or a twisted sandwich H-type dimer (D_1). This bathochromic shift is much more important than that observed in the absorption band (Figure 1), leading to an augmentation of the Stokes shift ($\Delta\nu_{st} = \nu_{abs} - \nu_{flu}$) with the loading (Table 1). The relatively small Stokes shift for the monomer (around 670 cm^{-1}) suggests a similar geometry and solvation-shell in the excited and in the ground states. However, the presence of different dimers of R6G in Lap films can contribute to red or blue spectral shifts in the absorption band depending on their geometries, and the formation of different dimers with overlapping bands would cause a widening in the global absorption band but not a neat absorption spectral shift (Figure 1).[45] Nevertheless, the highly efficient energy transfer to the lowest fluorescent excited state of the R6G aggregates would contribute to the significant red shift observed in the fluorescent band and with a relative low broadening (Table 1).[68]

The excitation spectra give out two absorption bands for the R6G dimers placed at lower and higher wavelengths than the absorption band of the R6G monomer (curves b−j against curve a in Figure 2B), the band at lower energies being more intense than that at higher energies. The excitation at this last excited state does not lead to a new hypsochromic shifted fluorescence band because a very fast nonradiative deactivation process could depopulate this state toward the lowest fluorescent excited state of the dimers. Therefore, the shape of the excitation spectra at the 1−22% CEC R6G/Lap loadings is consistent with an oblique head-to-tail dimer previously proposed by absorption data. However, the drastic decrease in the fluorescent emission of the monomers, and its corresponding excitation band, suggest an important energy transfer from the monomer locally excited state to a nonfluorescent low-lying excited state,[68] for instance to the first excited state of a H-type dimer.

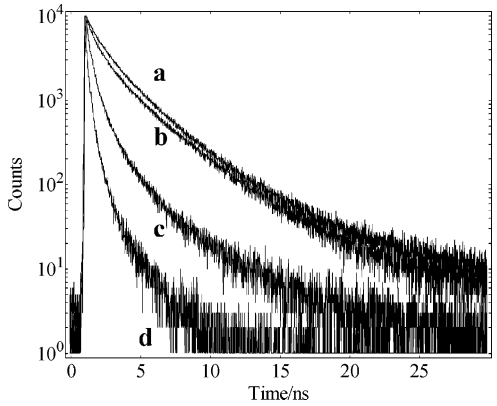

Figure 5. Fluorescence decay curves of R6G/Lap films at different dye loadings (in % CEC) at 550 nm after excitation at 410 nm: (a) 0.1%, (b) 1%, (c) 5.7%, and (d) 22%.

The shape of these excitation spectra reminds us of that previously calculated for the average absorption spectrum for the dimers in the 1−22% CEC loading range.[45] Figure 4 shows a representative illustration for the 5.7% CEC sample. The shoulder between the two excitation bands should be ascribed to the reminiscent contribution of the monomeric excitation band (curve a in Figure 2B). In fact, absorption data disclose the presence of monomeric units with a molar fraction about 0.5 for this sample;[45] a higher contribution of the monomeric excitation band should be expected in the recorded spectrum. This result suggests the important fluorescence quenching for the monomeric emission by the R6G dimers and that part of the fluorescent emission from the dimers is due to the direct excitation of the monomeric excited state (monomer-to-dimer excitation energy transfer).

The similarity in both spectra (Figure 4) indicates the goodness of the mathematical procedure developed to eliminate the monomer contribution for the recorded absorption spectra to determine the pure absorption spectra of the aggregates.[45] Besides, Figure 4 reveals an efficient excitation energy transfer from the highest excited state to the fluorescent lowest excited state of the dimers, since the relative intensity at 495 nm of both excitation and absorption bands is almost the same, i.e., the direct excitation at 495 nm to the monomer excited state and to the higher energy levels of the aggregate would populate the fluorescent lowest excited state of the aggregates by energy transfer and/or nonradiative internal conversion processes.

Figure 5 shows the evolution of the fluorescent decay curves of R6G/Lap films with the loadings. For moderate loadings (1−22% CEC range) all deconvoluted decay curves have to be analyzed with 4-exponential decays. The progressive diminution in the fluorescence lifetime is reflected in the average value of the lifetime data obtained from eq 2 and eq 3 and has been enclosed in Table 1. The decrease in the $\langle\tau_{flu}\rangle$ value with the loading does not quantitatively correlate with the decrease in the fluorescent efficiency (referred as the I_{flu}/A_{exc} parameter, Table 1); for instance, for the 5.7% CEC sample the $\langle\tau_{flu}\rangle$ value decreases 2.6 times respect to the monomer average lifetime, whereas the diminution in the I_{flu}/A_{exc} value is around 35 times. Moreover, the loss in the $\langle\tau_{flu}\rangle$ value (around 10 times) is not so pronounced as that in the I_{flu}/A_{exc} value (around 560) if the 22% CEC sample is compared with respect to the 0.1% CEC sample. These results suggest the existence of a static quenching process in R6G/Lap films, for instance, the formation of a sandwich H-type dimer. Thus, the direct excitation at 495 nm to the highest excited state of this H-type R6G dimer would be inactive in fluorescence, since the lowest excited state of H-type dimers are not fluorescent and act as traps of the excitation energy. In fact, H-type dimers of R6G formed in aqueous solutions are very efficient quenchers for the fluorescent emission of the monomer units.[67] Present results indicate that the proportion of H-type dimers over J-type dimers augments with the dye loading in the 1−25% CEC range. This conclusion agrees with the previously reported from absorption data,[45] where the relative intensity of the J-band over the H-band of the absorption spectrum of the aggregates decreases by increasing the dye loading.

Time-resolved fluorescence spectroscopy reveals a complicated emission for the fluorescent dimers of R6G in Lap films. Indeed, Figure 6A shows a slower deactivation process to the ground state at longer emission wavelengths. Consequently, the average lifetime of R6G dimers increases in the lower energy part of the fluorescence band for moderate (1−22% CEC) loading samples (Table 1); for instance, the average lifetime of the 5.7% CEC sample changes from 1.6 ns at 550 nm to 2.5 ns at 580 nm. This dependence of the average lifetime on the emission wavelength is not observed in highly concentrated dye/clay samples (>40% CEC), where higher-order aggregates of R6G were previously proposed by absorption spectra.[45] Present results should indicate a complex fluorescence behavior for moderate loadings, which could be attributed to different phenomena, such as energy transfer to or between dimers, nonhomogeneous distribution of R6G dimers in Lap films or, more probably, to the presence of several fluorescent R6G dimers with different emission properties. Those dimers with fluorescent emission at higher wavelengths would present longer lifetimes. This is confirmed by the TRES technique (Figure 6B), where a gradual shift of the fluorescence band to lower energies

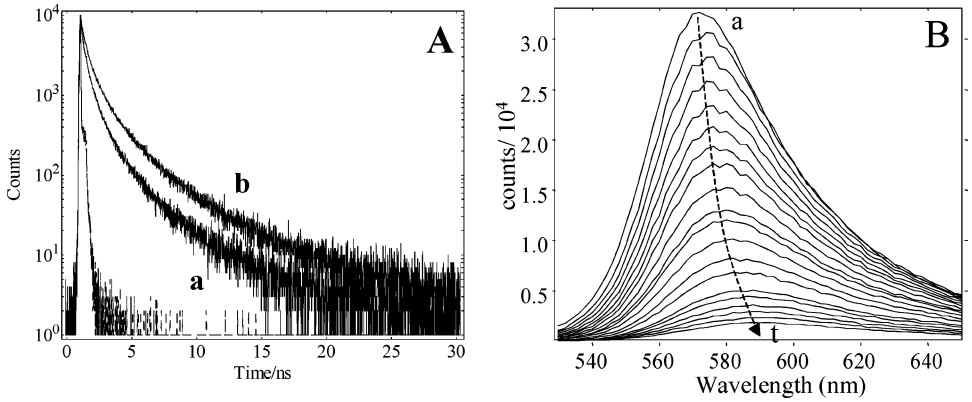

Figure 6. (A) Fluorescence decay curves for the 5.7% CEC sample recorded at different emission wavelengths: (a) 550 and (b) 580 nm. (B) Time-resolved emission spectra for the 22% CEC sample (see Figure 3 legend).

with the time after excitation is observed in this moderate 1−22% CEC loading range.

Present results of R6G/Lap films indicate a strong fluorescence quenching of the monomer emission band since the monomer band is not observed in the excitation spectrum of 1% CEC sample (curve b in Figure 2B), whereas absorption data suggest that more than 80% of R6G molecules are present as monomer units in this 1% CEC sample.[45] For this reason, the formation of fluorescent oblique head-to-tail dimers, with a relatively poor emission capacity, cannot explain the drastic diminution in the fluorescent intensity experimentally observed (Figure 2A). So the emission data corroborate the coexistence of different fluorescent and nonfluorescent R6G dimers in the Lap films. Sandwich H-type dimers, apart from their nonfluorescent character, act as traps for the excitation energy, being effective quenches of the fluorescent emission from monomers. The important Stokes shift (higher bathochromic shift in the emission band than in the absorption band) observed in the present systems confirms the coexistence of two different dimers: a nonfluorescent H-type aggregate and a fluorescent J-type dimer. Because of the gradual increase in the Stokes Shift with the loading (Table 1), the H-type dimer should be favored in high dye coverage films.

For high loading samples (>25% CEC), where higher-order aggregates of R6G Lap films were previously reported by absorption spectroscopy,[45] the fluorescence properties of R6G/Lap films become less complicated with respect to those in moderate loadings (1−25% CEC): a fluorescence band placed at around 600 nm is detected and the fluorescence decay curves can be perfectly analyzed by triexponential decay (versus 4-exponetial decays in moderate loadings), and the average lifetime is practically independent of the emission wavelength (Table 1). The average lifetime (around 1 ns) does not decrease so extensively as the fluorescent efficiency (I_{flu}/A_{exc}) with respect to the highest diluted R6G/Lap samples (<0.1% CEC) and it is even higher than the average lifetime of moderate samples (10−22% CEC, Table 1). These results would indicate a very low radiative deactivation rate constant for the high-order aggregates, drastically reducing the fluorescence quantum yield, but increasing the mean lifetime of the excited state with respect to those observed in moderate loadings (Table 1). This interpretation would be consistent with poor fluorescent twisted H-type higher-order aggregates previously proposed from absorption data.[45] Indeed, exciton theory indicates that the transition between the ground and the lowest excited state of a twisted H-type aggregate is not forbidden with a transition probability dependent on the twisted angle. Although the fluorescent emission of the H-type higher-order aggregates of R6G in Lap films are detectable, its fluorescence intensity is much lower than the monomer emission. For instance, the fluorescence intensity of the highest loading samples is around three orders of magnitude lower than the emission detected in the lowest loading films. TRES data indicate that the emission band of the long-lifetime high-order aggregates is around 610 nm (data nonshown).

Present results suggest that the twisted sandwich geometry of R6G aggregates at Lap films is favored at high loadings: increase in the Stokes shift with the loading (Table 1), drastic quenching in the fluorescent intensity with the loading (inset Figure 2A); and the significant increase in the relative intensity of the excitation band placed at higher energy (Figure 2B). This molecular arrangement allows a more compact distribution of the molecules, since head-to-tail aggregates need more space in the clay to be formed. For low dye concentrations the molecules disposed more parallely to the surface, but as the loading increases the molecules are disposed more perpendicularly to the surface of the film, in agreement with other authors,[21,22] favoring the stacking and compactness and therefore a sandwich distribution.

Conclusions

R6G laser dye intercalated in solid thin films of Lap clay shows interesting photoluminescence properties. R6G monomers in Lap films, observed in diluted loading samples (≤0.1% CEC), present fluorescent bands at around 548 nm with a higher emission capacity and lifetime than in liquid solutions. These results suggest a decrease in the nonradiative deactivation rate constants of R6G monomers in the solid films, probably due to a more rigid environment for the dye molecules in the inorganic matrix. These results confirm the validity of the incorporation of guest dyes into inorganic host materials to improve the photophysical properties of laser dyes. However, R6G molecules tend to self-aggregate in moderate dye loadings (1−25% CEC) and dimers reduce the fluorescent efficiency of R6G dye molecules in Lap films. Two or three different kinds of dimers can be distinguished: oblique head-to-tail J-type dimers (D_2 in Scheme), with weak fluorescence bands at around 575 nm, and twisted sandwich (D_1) and/or coplanar displaced (C with $\theta >$ 54.7°) H-type dimers, which both contribute to the quenching of the monomer emission. The proportion of the H-type dimers increases in detriment of the J-type dimers by increasing the relative R6G concentration in Lap films. Further increases in the dye loading (>40% CEC) lead to the formation of higher-order H-type aggregates, with a reminiscent fluorescence band at around 600 nm and a longer lifetime than that of J-type dimers.

Acknowledgment. This work is supported by the Spanish MEC Minister (Research Project MAT2004-04643-C03-02). V.M.M thanks the MECyD Minister for a research grant.

References and Notes

(1) Schulz-Ekloff, G.; Wöhrle, D.; Van Duffel, B.; Schoonheydt, R. A. *Microporous Mesoporous Mater.* **2002**, *51*, 91−138 and references therein.
(2) Reisfeld, R. *Optical Mater.* **2001**, *16*, 1−7.
(3) Nalwa, H. S., Ed. In *Handbook of Advaced Electronic and Photonic Materials and Devices*; Academic Press: San Diego, CA, 2001; Vol. 7.
(4) Calzaferri, G.; Huber, S.; Maas, H.; Minkowski, C. *Angew. Int. Ed. Engl.* **2002**, *42*, 3732−3758.
(5) Arena, A.; Patané, S.; Saitta, G.; Rizzo, G.; Galvano, S.; Neri, G. *J. Non-Crystalline Solids* **2003**, *331*, 263−268.
(6) Fukuda, M.; Kodama, K.; Yamamoto, H.; Mito, K. *Dyes Pigments* **2004**, *63*, 115−125.
(7) Spadavecchia, J.; Ciccarella, G.; Capone, S.; Rella, R. *Sensors Actuators B* **2004**, *100*, 88−93.
(8) Miled, O. B.; Grosso, D.; Sanchez C.; Livage, J. *J. Phys. Chem. Solids* **2004**, *65*, 1751−1755.
(9) Nardis, S.; Monti, D.; Natale, C.; D'Amico, A.; Siciliano, P.; Forleo, A.; Epifani, M.; Taurino, A.; Rella, R.; Paolesse, R. *Sensors Actuators B* **2004**, *103*, 339−343.
(10) Geng, Y.; Gu, D.; Gan, F. *Opt. Mater.* **2004**, *27*, 193−197.
(11) Lam, S. Y.; Damzen, M. J. *Appl. Phys. B* **2003**, *77*, 577−584.
(12) Schrader, S.; Penzkofer, A.; Holzer, W.; Velagapudi, R.; Grimm, B. *J. Lumin.* **2004**, *110*, 303−308.
(13) Pertermann, R.; Tian, M.; Tatsuura, S.; Furuki, M. *Dyes Pigments* **2003**, *57*, 43−54.
(14) Bandara, J.; Divarathne, C. M.; Nanayakkara, D. S. *Solar Energy Mater. Solar Cells* **2004**, *81*, 429−437.
(15) Fan, Q.; McQuillin, B.; Bardley, D. D. C.; Whitelegg, S.; Seddon, A. B. *Chem. Phys. Lett.* **2001**, *347*, 325−330.
(16) Dubois, A.; Canva, M.; Brun, A.; Chaput, F.; Boilot, J.-P. *Appl. Optics* **1996**, *35*, 3193−3199.
(17) Ramamurthy, V.; Eaton, F. D. *Chem. Mater.* **1994**, *6*, 1128−1136.
(18) bin Hussein, M. Z.; Zainal, Z.; Yahaya, A. H.; Aziz, A. B. A. *Mater. Sci. Eng.* **2002**, *B88*, 98−102.
(19) Fujita, T.; Iyi, N.; Kosugi, T. *Clays Clay Miner.* **1997**, *45*, 77−84.

(20) Mitzi, D. B. *Chem. Mater.* **2001**, *13*, 3283−3298.
(21) Ogawa, M.; Kuroda, K. *Chem. Rev.* **1995**, *95*, 399−438.
(22) Ogawa, M.; Kuroda, K. *Bull. Chem. Soc. Jpn.* **1997**, *70*, 2593−2618.
(23) Rurack, K.; Hoffman, K.; Al-Soufi, W.; Resch-Genger, U. *J. Phys. Chem. B* **2002**, *106*, 9744−9725.
(24) van Duffel, B.; Verbiest, T.; Van Elshocht, S.; Persoons, A.; De Schryver, F. C.; Schoonheydt, R. A. *Langmuir* **2001**, *17*, 1243−1249.
(25) Inoue, T.; Moriguchi, M.; Ogawa, T. *Thin Solid Films* **1999**, *350*, 238−244.
(26) Era, M.; Kobayashi, T.; Mitsuharu, N. *Current Appl. Phys.* **2005**, *5*, 67−70.
(27) Mannini, M.; Gambinossi, F.; Baglioni, P.; Caminati, G:, *Bioelectrochem.* **2004**, *63*, 9−12.
(28) Kim, D. W.; Blumstein, A.; Tripathy, S. K. *Chem. Mater.* **2001**, *13*, 1916−1922.
(29) Bockstette, M.; Wöhrle, D.; Braun, I.; Schulz-Ekloff, G. *Microporous Mesoporous Mater.* **1998**, *23*, 83−96.
(30) Miyamoto, N.; Kuruda, K.; Ogawa, M.; *J. Mater. Chem.* **2004**, *14*, 165−170.
(31) Ramamurthy, V., Ed. *Photochemistry in Organized and Constrain Media*; VCH: New York, 1991.
(32) Newmann, A. C. D. *Chemistry of Clays and Clay Minerals*; Longman Science Technology Mineral Society: London, 1987.
(33) Van Olphen, H. *An Introduction to Clay Colloid Chemistry*, Wiley: New York, 1977.
(34) Hagerman, M. E.; Salamone, S. J.; Herbst, R. W.; Payeur, A. L. *Chem. Mater.* **2003**, *15*, 443−450.
(35) Schoonheydt, R. *Clay Clays Miner.* **2002**, *50*, 411−420.
(36) Giannelis, E. P. *Chem. Mater.* **1990**, *2*, 627−629.
(37) Sasai, R.; Fujita, T.; Iyi, N.; Itoh, H.; Takagi, K.; *Langmuir* **2002**, *18*, 6578−6583.
(38) Iyi, N.; Fujita, t.; Deguchi, T.; Sota, T.; López Arbeloa, F.; Kitamura, K. *Appl. Clay Sci.* **2002**, *22*, 125−136.
(39) Sasai, R.; Iyi, N.; Fujita, T.; López Arbeloa, F.; Martínez Martínez V.; Takagi, K.; Itoh, H. *Langmuir* **2004**, *20*, 4715−4719.
(40) Drexhage, K. M. *In Dye Laser*, Schäfer, F. P., Ed.; Springer-Verlag: Berlin 1990; Vol 1, p 187.
(41) McRae, E. G.; Kasha, M. *Physical Process in Radiation Biology*; Academy Press: New York, 1964.
(42) Kasha, M.; Rawls, H. R.; El-Bayoumi, M. A. *Pure Appl. Chem.* **1965**, *11*, 371−392.
(43) Van Olphen, H.; Fripiat, J. J. *Data Handbook for Clay Minerals and other Non-Metallic Minerals*; Pergamon Press: London, 1979.
(44) Martínez, Martínez, V.; López Arbeloa, F.; Bañuelos Prieto, J:, Arbeloa López, T.; López Arbeloa, I. *Langmuir* **2004**, *20*, 5709−5717.
(45) Martínez, Martínez, V.; López Arbeloa, F.; Bañuelos Prieto, J:, Arbeloa López, T.; López Arbeloa, I. *J. Phys. Chem. B* **2004**, *108*, 20030−20037.
(46) Nishikiori, H.; Fujii, T. *J. Phys. Chem. B* **1997**, *101*, 3680−3687.
(47) Fujii, T., Nishikiori, H.; Tamura, T. *Chem. Phys. Lett.* **1995**, *233*, 424−429.
(48) Nishikiori, H.; Tanaka, N.; Fujii, T. *Res. Chem. Intermed.* **2000**, *26*, 469−482.
(49) Bergström, F.; Mikhalyov, I.; Hägglöf, P.; Wortmann, R.; Ny, T.; Johanson, L. B. *J. Am. Chem. Soc.* **2002**, *124*, 169−204.
(50) Lucia, L. A.; Yui, T.; Sasai, R.; Takagi, S.; Takagi, K.; Yoshida, H.; Whitten, D. G.; Inoue, H. *J. Phys. Chem. B* **2003**, *107*, 3789−3797.
(51) Vogel, R.; Meredith, P.; Harvey, M. D.; Rubinsztein-Dunlop, H. *Spectroichim. Acta A* **2004**, *60*, 245−249.
(52) del Monte, F.; Levy, D. *J. Phys. Chem. B* **1999**, *103*, 8080−8086.
(53) Vuorimaa, E.; Ikonen, M.; Lemmetyinen, H. *Chem. Phys.* **1994**, *188*, 289−302.
(54) Vuorimaa, E.; Belovolova, L. V.; Lemmetyinen, H. *J. Luminiscence* **1997**, *71*, 57−63.
(55) Tsukavona. V.; Lavoie, H.; Harata, A.; Ogawa, T.; Salesse, C. *J. Phys. Chem. B* **2002**, *103*, 8080−8086.
(56) López Arbeloa, F.; López Arbeloa, T.; Gil Lage, E.; López Arbeloa**,** I.; De Schryver, F. C. *J. Photochem. Photobiol. A* **1991**, *56*, 313−321.
(57) Ballet, P.; Van der Auweraer, M.; De Schryver, F. C. *J. Phys. Chem.* **1996**, *100*, 13701−13715.
(58) Ray, K.; Nakahara, H. *J. Phys. Chem. B* **2002**, *106*, 92−100.
(59) Rohatgi-Mukherjee, K. K. *Ind. J. Chem.* **1992**, *31A*, 500−511.
(60) López Arbeloa, I. *J. Photochem.* **1980**, *14*, 97−105.
(61) Van der Auweraer, M.; Verschuere, B.; De Schryver, F. C. *Langmuir* **1988**, *4*, 583−588.
(62) Pevenage, D.; Van der Auweraer, M.; De Schryver, F. C. *Langmuir* **1999**, *15*, 8465−8473.
(63) Wiederrecht, G. P.; Sandi, G.; Carrado, K. A.; Seifert, S. *Chem. Mater.* **2001**, *13*, 4233−4238.
(64) Giese, R. F.; Van Oss, C. J. In *Surfactant Science Series*; Hubbard, A. T., Ed.; Marcel Dekker: New York, 2002; Vol. 105.
(65) Lakowicz, J. R. *Principles of Fluorescence Spectroscopy*, 2d ed.; Kluwer Academic: New York, 1999.
(66) Valeur, B. *Molecular Fluorescence. Principles and Applications*; Wiley-VCH: Weinheim, 2002.
(67) López Arbeloa, F.; López Arbeloa, T.; López Arbeloa, I. *Trends Photochem. Photobiol.* **1994**, *3*, 145−155.
(68) Scheblykin, I. G.; Varnavsky, O. P.; Verbouwe, W.; De Backer, S.; Van der Auweraer, M.; Vitukhnovsky, A. G. *Chem. Phys. Lett.* **1998**, *282*, 250−256.